Systematic comparison of monoclonal versus polyclonal antibodies for mapping histone modifications by ChIP-seq

Michele Busby[#], Cathy Xue, Yossi Farjoun, Elizabeth Gienger, Ido Yofe, Adrianne Gladden, Chad Nusbaum and Alon Goren[#]

Abstract

The robustness of ChIP-seq datasets is highly dependent upon the antibodies used. Currently, polyclonal antibodies are the standard despite several limitations: they are non-renewable, vary in performance between lots, and need to be validated with each new lot. In contrast, monoclonal antibody lots are renewable and provide consistent performance. To increase ChIP-seq standardization, we investigated whether monoclonal antibodies could replace polyclonal antibodies. We compared monoclonal antibodies that target five key histone modifications (H3K4me1, H3K4me3, H3K9me3, H3K27ac and H3K27me3) to their polyclonal counterparts. Overall performance was highly similar for four monoclonal/polyclonal pairs. In contrast, the binding patterns for H3K27ac differed substantially between polyclonal and monoclonal antibodies. However, this was most likely due to the distinct immunogen used rather than the clonality of the antibody. Altogether, we found that monoclonal antibodies as a class perform as well as polyclonal antibodies. Accordingly, we recommend the use of monoclonal antibodies in ChIP-seq experiments.

Introduction

Chromatin immunoprecipitation followed by sequencing (ChIP-seq) is one of the major technologies for investigating chromatin structure on a genomic scale. In this technique, the histone proteins bound to DNA are cross-linked to the DNA. After DNA shearing, a specific antibody is used to enrich the targeted protein by immunoprecipitation, which also enriches the specific DNA it is bound to because it is cross-linked to it. Finally, the DNA fragments that precipitated with the enriched protein are sequenced. Hence, the results of each experiment are highly dependent upon the quality of the antibody that is used.

Polyclonal antibodies have been used as the standard antibody reagent for ChIP-seq by many labs and consortia (Consortium, 2012, Bernstein et al., 2010, Landt et al., 2012). Problematically, however, polyclonal antibody lots are a limited resource, as each lot is raised from a different immunized animal. Each polyclonal batch consists of a highly complex population of individual antibody molecules, representing the unique response of that animal's immune system. Some of these component antibody molecules will specifically target the epitope in question, but other molecules in this population may

enrich for other non-target proteins. Different batches raised to the same target epitope will thus naturally differ in performance and must be validated before use. Critically, once exhausted, a polyclonal antibody lot cannot be reproduced (Lipman et al., 2005). To overcome these limitations, many scientists have advocated for the use of monoclonal antibodies (Baker, 2015, Bradbury and Pluckthun, 2015, Soll, 2014), as these antibodies are harvested from purified cell lines derived from a single immune cell. Thus, all monoclonal antibody lots are uniform and consist of a single antibody species that specifically targets the desired epitope.

To investigate whether monoclonal antibodies can substitute for polyclonal antibodies in ChIP-seq procedures while retaining equivalent performance, we designed and carried out a direct side-by-side comparison. We compared a set of five monoclonal antibodies targeting key histone modifications (H3K4me1, H3K4me3, H3K9me3, H3K27ac, and H3K27me3) to their polyclonal counterparts. To ensure that all samples and antibodies were handled in a precisely controlled manner, all work was performed employing automated ChIP-seq protocols implemented on a standard laboratory liquid handling system.

As a class, we found that the performance of monoclonal antibodies in ChIP-seq assays was equal to that of polyclonal antibodies. Given that monoclonal antibodies represent a renewable resource, and eliminate the lot-to-lot variability that is expected with polyclonal antibodies, the replacement of polyclonal antibodies with monoclonal antibodies for use in ChIP-seq and similar affinity-based methods has significant benefits. Employing monoclonal antibodies will result in increased reproducibility and robustness and will substantially improve standardization of results among data sets.

Results

We designed an experimental system for rigorously comparing the performance of monoclonal and polyclonal antibodies in ChIP-seq and applied it to antibodies targeting five key histone modifications (H3K4me1, H3K4me3, H3K9me3, H3K27ac and H3K27me3) (**Table 1**). These epitopes

provide a rigorous test set of antibodies as they represent open and closed chromatin environments, have distinct localization patterns as described in **Table 2,** and are commonly used in studies of chromatin structure. We performed ChIP-seq with these antibodies in the human erythroleukemic cell line K562 using unenriched whole cell extract (WCE) as a control. To control for experimental variability, we implemented a fully automated ChIP-seq process (Garber et al., 2012) that ensures precise liquid handling, maximizes reproducibility, and controls for human error. We performed two to four technical replicates for each antibody tested to control for experimental variability and sequenced the libraries using Illumina paired-end reads. We then further computationally normalized our datasets to account for possible technical variability introduced by fragmentation and differing read depths. Finally, we analyzed our data to compare the performance of monoclonal and polyclonal antibodies focusing on the specificity and the number of peaks identified, as well as the overall pattern of reads localized across the genome.

Normalization of ChIP-seq datasets

Before analyzing our data, we computationally normalized the aligned reads to isolate the effects of each antibody from two possible issues that could confound the comparison: (**i**) A higher number of reads increases the power to distinguish peaks from background noise (Jung et al., 2014); (**ii**) Chromatin DNA has been shown to shear into different size fragments in regions of open versus closed chromatin, and genomic regions originating from open chromatin are more likely to shear into small fragments (Rozowsky et al., 2009). The combination of this shearing bias and a narrow size selection can lead to an artifactual enrichment of reads in areas of open chromatin leading to pile ups of reads that mimic peaks.

The effects of fragment length bias are therefore protocol-specific and dependent upon both the fragmentation method and size selection. To quantify the effect of fragmentation on the localization of reads in our protocol, we examined our WCE control data. First, we defined the regions as open or closed chromatin based on ENCODE mappings derived from the combined annotations of ChromHMM (Ernst and Kellis, 2012) and Segway (Hoffman et al., 2012). This mapping approach annotates the K562 genome according to seven canonical types: transcription start sites, promoter flanking regions,

enhancers, weak enhancers, CTCF-enriched elements, transcribed regions, and repressed regions. According to this mapping approach, the majority of the annotated K562 genome (84%) is in repressed regions (closed chromatin) while only ~1% of the K562 annotated genome is in transcription start sites (open chromatin).

Next, to assess the regional bias of the fragmentation of the cross-linked DNA, we quantified insert sizes of fragments falling into open and closed chromatin, expecting the insert size to be equivalent to the size of the DNA fragment originating in the immunoprecipitation step. To explore the effects of fragment length variation in our system, we examined reads with insert sizes between 70 and 700 bases, the size range of inserts typically found in an Illumina flow cell. We observed that the percentage of reads localizing to transcription start sites (TSS) was inversely correlated with the length of the insert size (R^2=0.80) with a 2.6 fold higher percentage of reads localizing to TSS in read pairs with shorter (70-120bp) versus longer (650-700bp) insert sizes. Reads localizing to repressed regions were positively correlated with insert size (R^2=0.70) though the difference in coverage is only 5% (**Supplemental Figure 1**).

While we have optimized our shearing process to provide high reproducibility of the fragmentation process (**Methods**), since each sample is sheared separately, the fragmentation might vary between samples. To account for potential differences in fragmentation, we randomly selected alignments so that each aligned read set for a given histone modification had the same number of reads and fragment size distribution (**Table 1**). As the insert size is equal to the length of the DNA fragment in the original pool, this normalization method approximates experiments that have both the same fragmentation and read depth. Because normalizing by insert size could also obscure true differences between antibodies, parallel analyses using alignments randomly sampled to the lowest read count in the group are included as supplementary figures for key results.

Comparison of peaks between ChIP-seq datasets

We investigated the relative performance of the antibodies in terms of sensitivity, specificity, and the number and distribution of peaks. Initial visualization of the data in a genome browser revealed a high degree of similarity in read coverage between monoclonal and polyclonal antibodies (**Figure 1**).

The best performing antibodies are those that provide the highest enrichment for DNA fragments associated with the target protein. However, a greater portion of reads localizing to observed peaks could be indicative of either higher sensitivity of the antibody for its epitope or the addition of false peaks resulting from a higher degree of non-specific binding. To quantify antibody performance, we evaluated whether the monoclonal and polyclonal antibodies differed in the number of peaks identified or the percentage of reads that are in locations identified as peaks (Signal Portion of Tags – SPOT score (John et al., 2011)). Peaks were called for each sample using the HOMER software (Heinz et al., 2010) with WCE data used as the control. For H3K27ac, H3K27me3, H3K4me3, and H3K9me3 the polyclonal antibody had a significantly higher number of peaks called versus their monoclonal counterparts ($p<0.05$ by t-test, **Table 2** and **Supplemental Figure 2A**). However, only the polyclonal antibodies to H3K27me3 and H3K4me3 had significantly higher percentage of reads in the peak regions ($p<0.05$, **Table 2** and **Supplemental Figure 2B**).

To assess the specificity of binding, we tested whether reads and peaks were mapped to their expected regions. **Figure 2** and **Supplemental Figure 3A** show the number of peaks that mapped to each of the seven ENCODE canonical regions for each antibody. While results between the monoclonal and polyclonal antibodies for each epitope were similar, a greater percentage of reads mapped to their expected regions of the genome (**Table 1**) for the monoclonal samples of H3K27ac (88.1% mono vs. 80.2% poly, $p<0.01$). Due to the low variability between technical replicates in our system, small differences also reached statistical significance for H3K4me3 (92.8% mono, 91.5% poly, $p<0.01$) and H3K27me3 (98.2% mono and 98.4% poly, $p=0.04$). These findings are consistent with the numbers of reads mapping to these regions (**Supplemental Figure 3B** and **C**). We note that this approach – evaluating the percentage of reads mapped to ENCODE canonical genomic regions – does not provide a

fully orthogonal validation of the specificity of the antibodies as the annotations were themselves created from ChIP-seq data.

Next, we tested whether the locations of peaks called were consistent between monoclonal and polyclonal antibodies by comparing which peaks in one sample overlapped peaks identified in another sample. As expected, the overall percentage of peaks that overlap was high (60-86%) for the histone modifications associated with open chromatin (H3K27ac, H3K4me1, and H3K4me4) but substantially lower (11-27%) for histone modifications associated with closed chromatin (H3K9me3 and H3K27me3). This difference is most likely due to the fact that repressed regions make up the largest portion of the genome and deeper sequencing is required to comprehensively map these marks. This lack of power makes it less likely that peaks that are identified in one sample will also be identified in a second sample. For most of the epitopes, the overlap of peaks called in ChIP-seq datasets from either monoclonal or polyclonal antibodies was similar to the overlap of peaks called using the same antibody (**Table 3**). Consistent with other data, the H3K27ac antibodies showed a high reproducibility of technical replicates using the same antibody (85-86% overlap), but showed a lower degree of reproducibility when comparing samples prepared with the monoclonal antibody to those prepared with the polyclonal antibody (79% overlap).

Whole Genome Read Coverage

We next investigated the binding patterns of reads across the entire genome. To provide a basis for this quantitative evaluation, we defined non-overlapping bins of 2000 base pairs across the genome and counted the reads falling into each bin. We first compared the correlations in technical replicates in the samples normalized by insert size versus those normalized by random sampling. Correlations were highly similar, indicating that fragmentation and size selection were well controlled in these samples and did not introduce a significant source of bias (**Figure 3** and **Supplemental Figure 4**).

For all antibodies except H3K27ac the correlations between monoclonal and polyclonal antibodies were similar to those observed between technical replicates using the same antibody (**Figure 3** and **Supplemental Figure 4**).

Next, we examined the differences between the H3K27ac monoclonal and polyclonal samples more closely. The H3K27ac modification is present both at enhancer regions and transcription start site regions (Zhou et al., 2011). Therefore, we compared the number of reads aligning in each region. Interestingly, we found that in datasets derived from the polyclonal H3K27ac antibody a higher number of reads fell into enhancer site regions relative to transcription start site regions when compared to the datasets derived from the monoclonal H3K27ac antibody (**Figure 4A**).

One possible explanation for this finding is that the polyclonal reagent, as it is a mix of individual antibody molecules, contains antibodies to multiple epitopes, one of which is enhancer-specific and increases the antibody's binding in this region. To examine this possibility, we performed ChIP-seq comparing three H3K27ac antibodies: the monoclonal and polyclonal mentioned above which were produced by Cell Signaling Technology (CST) and Active Motif, respectively, and a second monoclonal antibody obtained from Active Motif. We repeated this ChIP-seq experiment with the CST monoclonal and polyclonal antibody using HeLa cells and obtained the same pattern (**Figure 4B**). However, when we compared the Active Motif polyclonal antibody to the Active Motif monoclonal antibody the effect was not present. Instead, the ChIP-seq results from the monoclonal Active Motif antibody more closely resembled the polyclonal data (**Figure 4B**).

We were not able to obtain the sequences of the polypeptide immunogens that were used to raise these antibodies as the vendors consider these proprietary. However, the Active Motif antibodies were raised by two different immunogens having an overlapping amino acid sequence (disclosed by Active Motif's Technical Support to assist with understanding of the data generated for this project). These immunogens likely differed from the one used by Cell Signaling Technology.

Experimental quality control

To ensure that our ChIP-seq results were representative of the quality of the antibody rather than differences in the performance of the libraries or experiments, one replicate of the H3K27me3 polyclonal antibody was removed as it did not pass our quality control and differed substantially from the other three technical replicates (**Supplemental Figure 5**). Specifically, the number of reads falling into regions of transcription start sites was systematically higher in this replicate than in other replicates. A monoclonal replicate of the H3K4me1 and a monoclonal replicate of H3K9me1 failed to yield an adequate number of reads to be used in analysis. These samples were rerun in duplicate and each was replaced with two replicates.

Discussion

Our goal in designing this study was to improve current ChIP-seq procedures by increasing the reproducibility between experiments within the community, as well as enhance the usage of reagents that have long-term accessibility. Specifically, we explored whether monoclonal antibodies could properly replace the polyclonal antibodies routinely used in ChIP-seq.

Our experimental setup allowed us to directly compare performance of ChIP-seq carried out using both antibody types. Additionally, sequencing our data with paired-end reads allowed us to normalize alignments to eliminate fragmentation and size selection biases as confounding factors. As we observed a high degree concordance between results from data normalized by insert size and results from data randomly downsampled, differences in fragmentation and size selection did not appear to be a strong confounder in this experiment. However, it is possible that this issue may be a confounder in other applications. Here we further demonstrated that the insert length of paired-end reads was correlated with the genomic regions from which the fragments originated, consistent with earlier reports (Rozowsky et al., 2009). Further, we note that paired-end reads provide the only definitive way to assess the distribution of DNA fragment lengths that were ultimately sequenced. We therefore strongly recommend optimizing

fragmentation and size selection protocols to include the full range of genomic fragment sizes to avoid bias, as well as using paired-end reads for ChIP-seq experiments. In the future, it would be useful to evaluate whether insert size normalization can provide a cost-effective alternative to using WCE controls, particularly in experiments whose primary focus is to measure changes in protein binding under different conditions rather than an exhaustive mapping of binding locations.

Among the five antibodies tested, the polyclonal antibodies to H3K4me3 and H3K27me3 appeared to offer slightly higher sensitivity while the monoclonal antibody to H3K27ac appeared to offer higher specificity. However, given that the differences we saw between the H3K27ac monoclonal and polyclonal antibody were also seen in a second monoclonal antibody, these differences more likely result from the specific immunogen against which the antibody was raised rather than the mono- or polyclonality of the antibody. Because higher sensitivity was not seen in the other polyclonal antibodies, our results demonstrate that the use of monoclonal antibodies for ChIP-seq did not present any systematic disadvantage relative to polyclonal antibodies, and have the clear advantage of superior reproducibility. This conclusion is supported by high correlation in genome-wide and region-specific read counts between monoclonal and polyclonal antibodies, as well as the high degree of overlap in peak locations. Therefore, we suggest that usage of monoclonal antibodies for ChIP-seq experiments provides a key improvement over polyclonal ones.

Overall, our data are consistent with a model suggested by Peach and colleagues (Peach et al., 2012) in which some antibodies are better described as indicators of canonical regions of the genome rather than as markers of specific modifications. For instance, in our comparison of H3K27ac antibodies, the monoclonal and polyclonal antibodies displayed significant differences in their relative ratio of reads localized to putative enhancers versus transcription start sites. If we assume that the targeted acetylated H3K27 is the same molecule in each region, then the ability of the antibodies to identify H3K27ac was affected not just by the presence of the target but also by its local environment. Characteristics of the environment will determine the accessibility of the epitope to the antibody and the potential for off-target

binding. The pattern of the binding of a single antibody should thus be thought of as a collection of component parts that describe more than just the binary presence or absence of a modification. This inherent complexity is further complicated by the fact that researchers often do not know the precise nature of the immunogen that was used to raise a specific antibody because the antibody's producer holds this information as proprietary.

Thus, ChIP-seq datasets targeting the same epitope but using different antibodies cannot be considered directly comparable without substantial experimental validation. Standardizing on monoclonal antibodies would not only eliminate the batch-to-batch variability that is expected in polyclonal antibodies but would also increase the value of ChIP-seq datasets by allowing for more reliable reuse of existing datasets. Further, it would simplify the interpretation of ChIP-seq data by removing the added complexity that is introduced by using a polyclonal antibody that targets an unknown number of epitopes on the antigen.

The relative portion of reads aligned to different canonical regions of the genome was also affected by experimental variability. By examining the relative proportion of reads mapping to canonical regions of the genome, we were able to easily identify an outlier replicate in our K27me3 data that would have passed less rigorous quality screens. This finding demonstrates not only that replicates are imperative in any ChIP-seq experiment, but also that performing this simple analysis can provide valuable information for quality control.

Methods

Chromatin Immunoprecipitation (ChIP)

ChIP comprises the basic steps of crosslinking DNA to protein, shearing DNA, and pulling-down of the protein of interest by immunoprecipitation. Washes and mixes were conducted using the Bravo liquid handling platform (Agilent model 16050-102, "Bravo"). For the compositions of the buffers used, see (Ram et al., 2011); for the specific protocol for the Bravo, see (Garber et al., 2012).

Table 1 presents the antibodies used in this study. The polyclonal antibodies were previously assessed for accuracy by comparison to "gold standard" ENCODE data.

Crosslinking and DNA Shearing: K562 mylogenous leukemia cells (ATCC CCL-243) were cross-linked with formaldehyde as previously described (Ram et al., 2011). Fixed cell pellets (20 million cells each) were resuspended in lysis buffer and ChIP dilution buffer and incubated on ice to lyse the cells. Samples were then split across a 96-well plate. DNA shearing was conducted using a Covaris sonifier (model E220) at 4°C for 6 cycles of 1 minute, with these parameters DF-10%, PIP-175W, CPB-200. After sonication, the cell lysates were diluted 1:10 with ChIP dilution buffer. Roughly 50 μL of the cell lysate was set aside for use as the whole cell extract (WCE) control.

Bead Preparation: Immunoprecipitation was performed using magnetic beads coupled to antibodies by Protein A or Protein G linkers. The beads were prepared as follows: equal quantities of Protein A and Protein G Dynabeads (Invitrogen, 100-02D and 100-07D, respectively) were mixed, separated into 50 μL aliquots in a well plate, and washed twice with blocking buffer. The beads and antibodies, mixed and suspended in blocking buffer, were incubated in a cold room (4 °C) on a rotator for at least two hours to allow conjugation.

Immunoprecipitation of Target Protein and DNA Purification: Washed bead-antibody conjugates were added to the chromatin lysate and incubated overnight. At this point, the WCE was added to the

sample plate. Samples were washed six times with RIPA buffer, twice with RIPA buffer supplemented with 500 mM NaCl, twice with LiCl buffer, twice with TE, and then eluted in ChIP elution buffer to unlink and purify the DNA.

Library Construction

The library construction phase of ChIP-seq comprises DNA end-repair, A-base addition, adaptor ligation, and enrichment. Solid-Phase Reversible Immobilization (SPRI) cleanup was performed on the reverse-crosslinked DNA before library construction and after each of its four steps to remove proteins and other molecules.

SPRI Cleanup Protocol: SPRI cleanup steps were conducted using the Bravo, following protocols described by (Garber et al., 2012). All enzymes used in library construction were obtained from New England Biolabs. The initial and final SPRI cleanups for the reverse-cross-linked DNA were performed as follows: SPRI beads (Agencourt AMPure XP) were added to the unlinked DNA samples. The beads were washed on a 96-well bar magnet (ThermoFisher, catalog number: 12027) with 70% ethanol and air-dried. The DNA was eluted in 10 mM Tris-HCl buffer. Intermediate SPRI cleanups in the library construction process were conducted in the same manner. The SPRI beads in the reaction were reused to capture the DNA via addition of a 20% PEG solution.

End-Repair and A-base Addition: DNA end-repair was performed by adding T4 PNK enzyme and T4 polymerase to each well, followed by incubation at 12 °C for 15 minutes and at 25 °C for another 15 minutes. Following SPRI clean up, A-base addition was performed by adding Klenow 3' → 5' exonuclease and incubation at 37 °C for 30 minutes.

Adapter Ligation: Adapter ligation was performed by adding DNA ligase and PE Indexed oligonucleotide adapters to samples followed by incubation at 25 °C for 15 minutes. After the subsequent SPRI cleanup, eluted DNA was separated from the SPRI beads using a 96-well bar magnet for PCR enrichment.

Enrichment: DNA samples were PCR amplified at 95 °C for 2 minutes; 16 cycles of: 95 °C for 30 seconds, 55 °C for 30 seconds, 72 °C for 60 seconds; and 72 °C for 10 minutes.

Data Collection and Analysis

DNA fragments were processed by 2x25 paired-end or 2x37 paired-end sequencing (Illumina HiSeq 2500 or NextSeq 500, respectively).

To assess reproducibility, we designed an analysis pipeline consisting of the following steps: alignment, normalization, pairwise correlation and clustering, peak calling, and analysis. Reads were aligned by the Broad Genomics Platform using BWA (v5.9) (Li & Durbin, 2009).

To allow for meaningful comparisons between different samples, duplicate reads were removed from the alignment data (BAM file) and all alignment files for each epitope were downsampled using C++ scripts built using the BamTools API (Barnett et al., 2011). Scripts are available on GitHub (https://github.com/mbusby/).

Downsampling normalization by insert size was performed as follows: The program first counts how many read pairs are present for each insert size for each of a set of aligned files. We then select the lowest read count for each insert size from among the set of alignments. For example, if four alignments for a given antibody have one, two, three, and four million reads with an insert size of 100, all four alignments would be randomly sampled so that the four normalized alignments each have about one million reads with an insert size of 100. This is performed for each insert size present in all of the alignments in the group to yield final bam files with about the same number of reads and insert size distribution. This approach therefore allows for identical insert size distributions while maximizing the number of reads included in the output files. All samples for each histone modification were sampled as a group. The WCE control was not randomly sampled, nor were the HeLa samples due to their low starting read coverage.

Peaks were called using HOMER (v.4.5) (Heinz et al., 2010) with the whole cell extract (WCE) as a control under the default settings for paired-end reads using "histone" as the peak type.

We counted the number of peaks mapping to the canonical genomic regions using the BEDtools intersect tool, version 2.25 (Quinlan, 2014). To avoid counting peaks that overlapped annotation boundaries twice, we required that at least 60% of the peak region would overlap the annotated region. We used the BEDtools coverage tool to count the number of reads mapping to genomic regions. The combined Segway and ChromHMM annotation was downloaded from (Wilder and Dunham).

Acknowledgements

This work was supported by The Broad Institute SPARC (Scientific Projects to Accelerate Research and Collaboration) program. We would like to thank Charles Epstein and Chip Stewart at the Broad Institute for helpful discussions.

Figure legends:

Figure 1. Read coverage across the genome. IGV browser (Robinson et al., 2011, Thorvaldsdottir et al., 2013) generated images of tiled data files (TDFs) displaying the density tracks of reads aligned across the genome. The tracks show the correspondence in read coverage in monoclonal and polyclonal antibodies over representative genomic loci. **A**. Chromosome 7: 44,829,782-44,930,648 (about 100Kb), shows the read coverage of histone modifications associated with 'active chromatin' (H3K4me1, H3K4me3 and H3K27ac). The correspondence of in read coverage of **B.** H3K27me3 (Chromosome 22:19,492,023-19,849,594 (about 350Kb)), and **C.** H3K9me3 (Chromosome 19: 51,746,058-53,362,194 (about 1.6Mb)), two major histone modifications associated with repression.

Figure 2. Reads in peaks mapping to canonical chromatin regions of the genome as defined by the ENCODE mappings. This plot displays the percentage of reads that map to each canonical genome region. The canonical genome regions were defined by the combined ENCODE mapping and are abbreviated as follows: CTCF-enriched elements (*CTCF*), promoter flanking regions (*PF*), transcription start sites (*TSS*), transcribed regions (*T*), enhancers (*E*), weak enhancers (*WE*), and repressed regions (*R*). Only reads that were located at regions identified as peaks were used for this plot. For each peak dataset the reads were normalized by insert size.

Figure 3. Correlation between monoclonal and polyclonal antibodies across the genome. Scatter plots (Loglog) presenting counts of reads per bin in non-overlapping 2000 bp windows tiled throughout the genome in replicates of the monoclonal antibody (**left**; gray), the polyclonal antibody (**right**; gray), and polyclonal versus monoclonal (**center**; blue). The H3K27ac data (**A**) show divergence between polyclonal and monoclonal antibodies, while the H3K27me3 data (**B**) show that the reproducibility is nearly indistinguishable from the reproducibility of data derived from technical replicates using the same antibody.

Figure 4. Variability in H3K27ac patterns is dependent on the immunogen. A. Scatter plots where each point represents the count of reads aligning to a non-overlapping, variably-sized region as annotated

in the chromatin regions determined by ENCODE mapping of the genome. Values are summed for the replicates of monoclonal and polyclonal H3K27ac antibodies. The red line (on the left and right plots) represents slope=1. **B.** H3K27ac antibodies in HeLa cells.

References

BAKER, M. 2015. Reproducibility crisis: Blame it on the antibodies. *Nature,* 521**,** 274-6.

BARNETT, D. W., GARRISON, E. K., QUINLAN, A. R., STROMBERG, M. P. & MARTH, G. T. 2011. BamTools: a C++ API and toolkit for analyzing and managing BAM files. *Bioinformatics,* 27**,** 1691-2.

BERNSTEIN, B. E., STAMATOYANNOPOULOS, J. A., COSTELLO, J. F., REN, B., MILOSAVLJEVIC, A., MEISSNER, A., KELLIS, M., MARRA, M. A., BEAUDET, A. L., ECKER, J. R., FARNHAM, P. J., HIRST, M., LANDER, E. S., MIKKELSEN, T. S. & THOMSON, J. A. 2010. The NIH Roadmap Epigenomics Mapping Consortium. *Nat Biotechnol,* 28**,** 1045-8.

BRADBURY, A. & PLUCKTHUN, A. 2015. Reproducibility: Standardize antibodies used in research. *Nature,* 518**,** 27-9.

CONSORTIUM, E. P. 2012. An integrated encyclopedia of DNA elements in the human genome. *Nature,* 489**,** 57-74.

ERNST, J. & KELLIS, M. 2012. ChromHMM: automating chromatin-state discovery and characterization. *Nat Methods,* 9**,** 215-6.

GARBER, M., YOSEF, N., GOREN, A., RAYCHOWDHURY, R., THIELKE, A., GUTTMAN, M., ROBINSON, J., MINIE, B., CHEVRIER, N., ITZHAKI, Z., BLECHER-GONEN, R., BORNSTEIN, C., AMANN-ZALCENSTEIN, D., WEINER, A., FRIEDRICH, D., MELDRIM, J., RAM, O., CHENG, C., GNIRKE, A., FISHER, S., FRIEDMAN, N., WONG, B., BERNSTEIN, B. E., NUSBAUM, C., HACOHEN, N., REGEV, A. & AMIT, I. 2012. A high-throughput chromatin immunoprecipitation approach reveals principles of dynamic gene regulation in mammals. *Mol Cell,* 47**,** 810-22.

HEINZ, S., BENNER, C., SPANN, N., BERTOLINO, E., LIN, Y. C., LASLO, P., CHENG, J. X., MURRE, C., SINGH, H. & GLASS, C. K. 2010. Simple combinations of lineage-determining transcription factors prime cis-regulatory elements required for macrophage and B cell identities. *Mol Cell,* 38**,** 576-89.

HOFFMAN, M. M., BUSKE, O. J., WANG, J., WENG, Z., BILMES, J. A. & NOBLE, W. S. 2012. Unsupervised pattern discovery in human chromatin structure through genomic segmentation. *Nat Methods,* 9**,** 473-6.

JOHN, S., SABO, P. J., THURMAN, R. E., SUNG, M. H., BIDDIE, S. C., JOHNSON, T. A., HAGER, G. L. & STAMATOYANNOPOULOS, J. A. 2011. Chromatin accessibility pre-determines glucocorticoid receptor binding patterns. *Nat Genet,* 43**,** 264-8.

JUNG, Y. L., LUQUETTE, L. J., HO, J. W., FERRARI, F., TOLSTORUKOV, M., MINODA, A., ISSNER, R., EPSTEIN, C. B., KARPEN, G. H., KURODA, M. I. & PARK, P. J. 2014. Impact of sequencing depth in ChIP-seq experiments. *Nucleic Acids Res,* 42**,** e74.

LANDT, S. G., MARINOV, G. K., KUNDAJE, A., KHERADPOUR, P., PAULI, F., BATZOGLOU, S., BERNSTEIN, B. E., BICKEL, P., BROWN, J. B., CAYTING, P., CHEN, Y., DESALVO, G., EPSTEIN, C., FISHER-AYLOR, K. I., EUSKIRCHEN, G., GERSTEIN, M., GERTZ, J., HARTEMINK, A. J., HOFFMAN, M. M., IYER, V. R., JUNG, Y. L., KARMAKAR, S., KELLIS, M., KHARCHENKO, P. V., LI, Q., LIU, T., LIU, X. S., MA, L., MILOSAVLJEVIC, A., MYERS, R. M., PARK, P. J., PAZIN, M. J., PERRY, M. D., RAHA, D., REDDY, T. E., ROZOWSKY, J., SHORESH, N., SIDOW, A., SLATTERY, M., STAMATOYANNOPOULOS, J. A., TOLSTORUKOV, M. Y., WHITE, K. P., XI, S., FARNHAM, P. J., LIEB, J. D., WOLD, B. J. & SNYDER, M. 2012. ChIP-seq guidelines and practices of the ENCODE and modENCODE consortia. *Genome Res,* 22**,** 1813-31.

LIPMAN, N. S., JACKSON, L. R., TRUDEL, L. J. & WEIS-GARCIA, F. 2005. Monoclonal versus polyclonal antibodies: distinguishing characteristics, applications, and information resources. *ILAR J,* 46**,** 258-68.

PEACH, S. E., RUDOMIN, E. L., UDESHI, N. D., CARR, S. A. & JAFFE, J. D. 2012. Quantitative assessment of chromatin immunoprecipitation grade antibodies directed against histone modifications reveals patterns of co-occurring marks on histone protein molecules. *Mol Cell Proteomics,* 11**,** 128-37.

QUINLAN, A. R. 2014. BEDTools: The Swiss-Army Tool for Genome Feature Analysis. *Curr Protoc Bioinformatics,* 47**,** 11 12 1-11 12 34.

RAM, O., GOREN, A., AMIT, I., SHORESH, N., YOSEF, N., ERNST, J., KELLIS, M., GYMREK, M., ISSNER, R., COYNE, M., DURHAM, T., ZHANG, X., DONAGHEY, J., EPSTEIN, C. B., REGEV, A. & BERNSTEIN, B. E. 2011. Combinatorial patterning of chromatin regulators uncovered by genome-wide location analysis in human cells. *Cell,* 147**,** 1628-39.

ROBINSON, J. T., THORVALDSDOTTIR, H., WINCKLER, W., GUTTMAN, M., LANDER, E. S., GETZ, G. & MESIROV, J. P. 2011. Integrative genomics viewer. *Nat Biotechnol,* 29**,** 24-6.

ROZOWSKY, J., EUSKIRCHEN, G., AUERBACH, R. K., ZHANG, Z. D., GIBSON, T., BJORNSON, R., CARRIERO, N., SNYDER, M. & GERSTEIN, M. B. 2009. PeakSeq enables systematic scoring of ChIP-seq experiments relative to controls. *Nat Biotechnol,* 27**,** 66-75.

SOLL, D. R. 2014. The Developmental Studies Hybridoma Bank, a national resource created by the National Institutes of Health. How does it work? *MATER METHODS,* 4**,** 876.

THORVALDSDOTTIR, H., ROBINSON, J. T. & MESIROV, J. P. 2013. Integrative Genomics Viewer (IGV): high-performance genomics data visualization and exploration. *Brief Bioinform,* 14**,** 178-92.

WILDER, S. & DUNHAM, I. Available: http://genome.ucsc.edu/cgi-bin/hgTrackUi?db=hg19&g=wgEncodeAwgSegmentation.

ZHOU, V. W., GOREN, A. & BERNSTEIN, B. E. 2011. Charting histone modifications and the functional organization of mammalian genomes. *Nat Rev Genet,* 12**,** 7-18.

Figure 1.

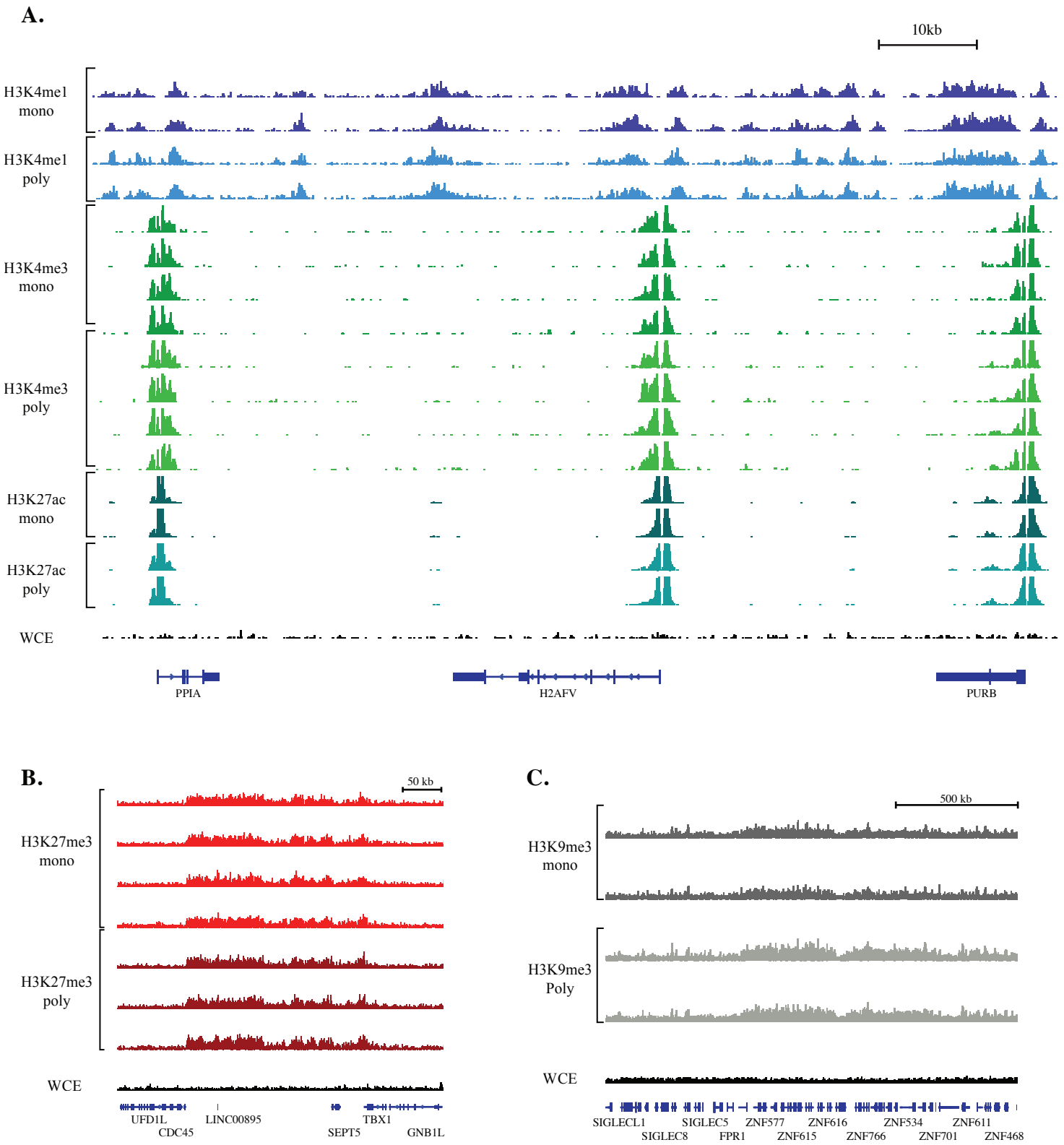

Figure 2.

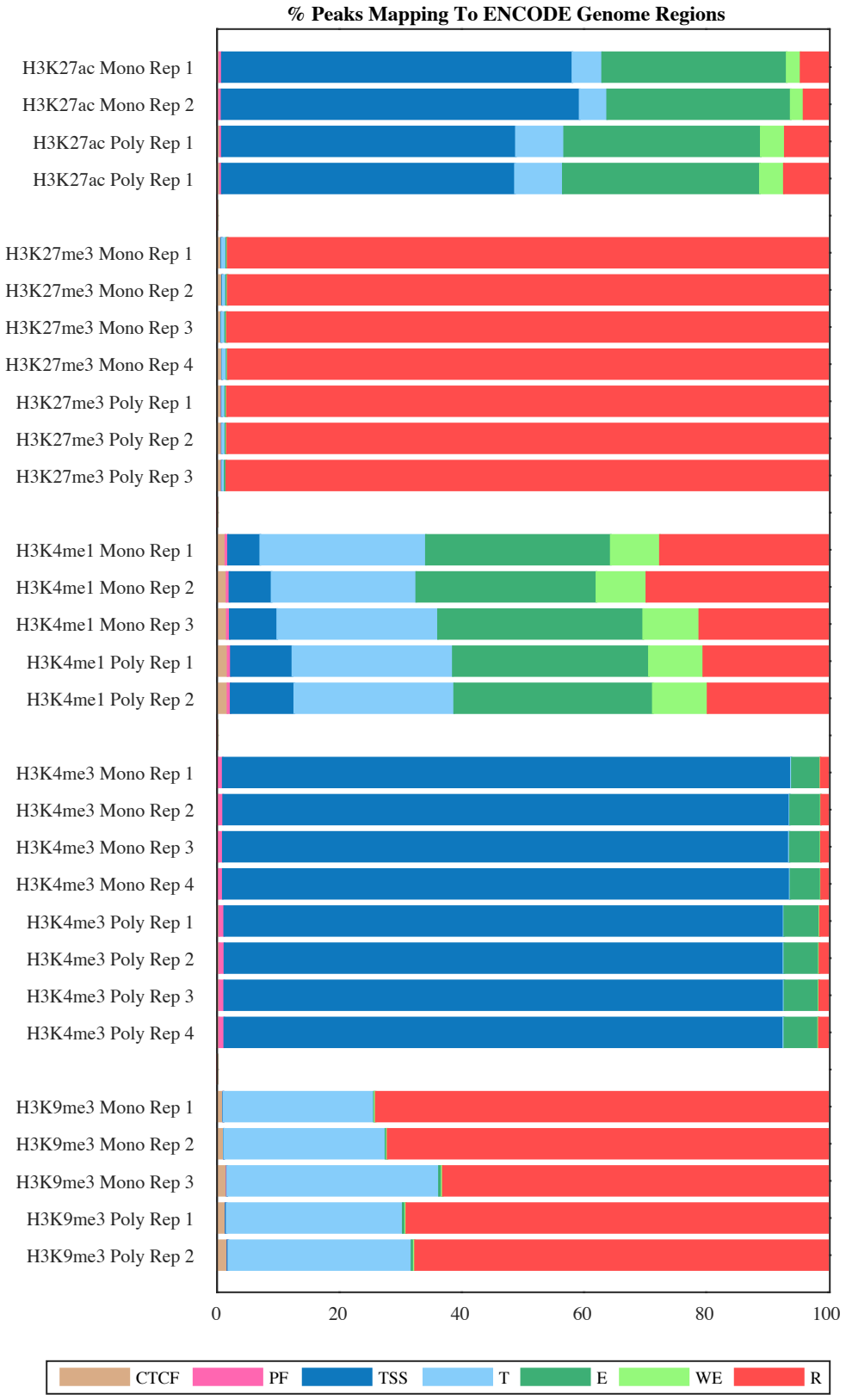

Figure 3.

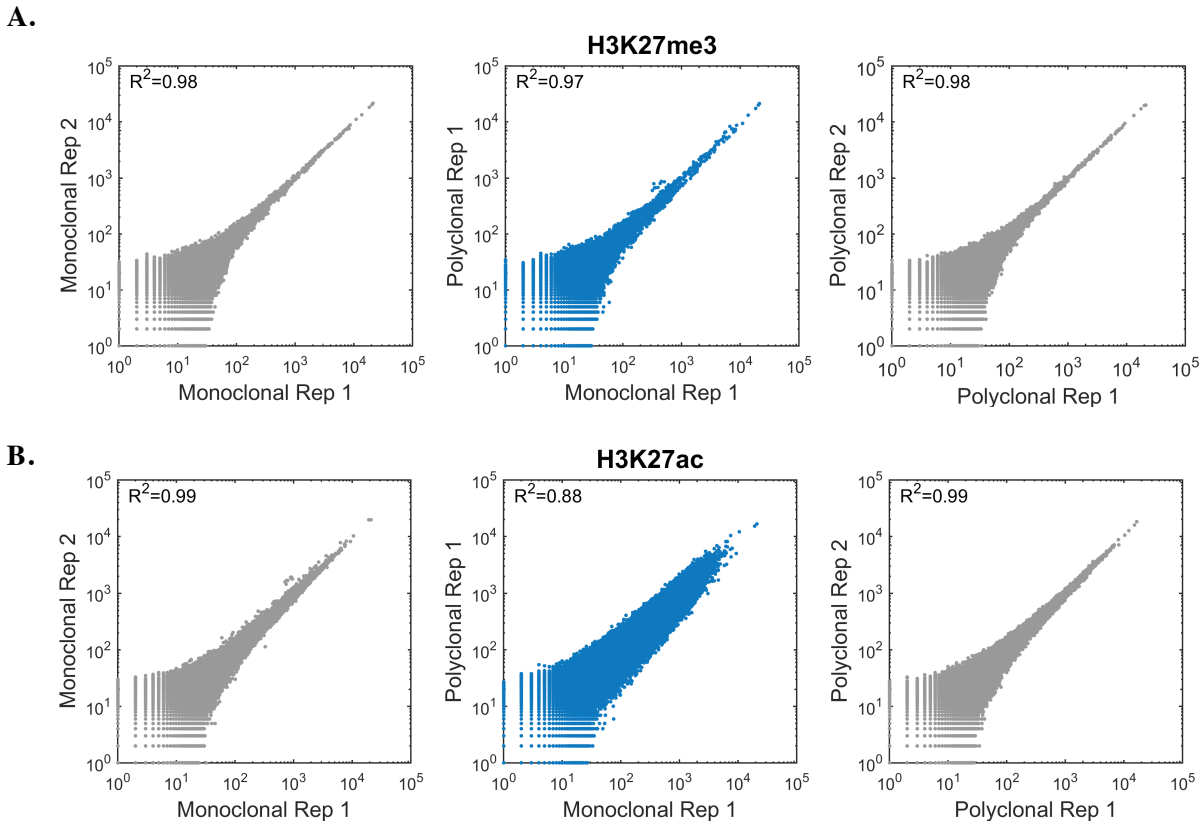

Figure 4.

A.

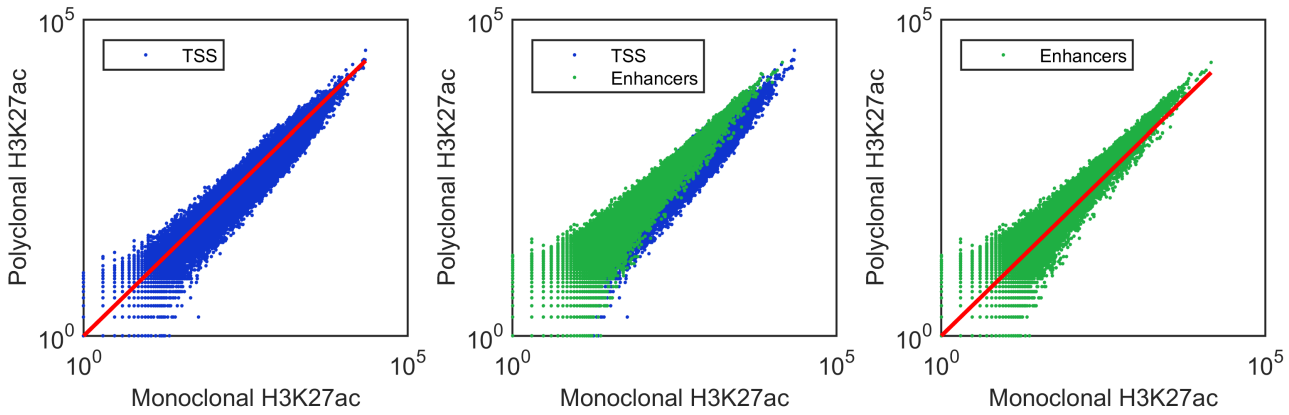

B.

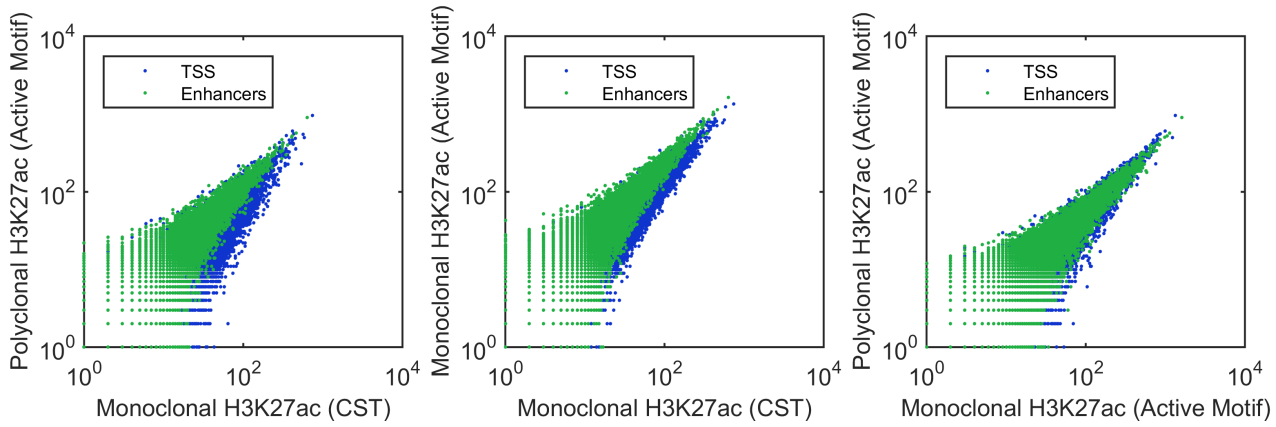

Table 1: Antibodies used in the study.

Epitope	Antibody Type	Commercial company	Catalog number
H3K4me1	Monoclonal	CST (Cell Signaling Technology)	5326
H3K4me1	Polyclonal	Active Motif	39297
H3K4me3	Monoclonal	CST	9751
H3K4me3	Polyclonal	Millipore	17-614
H3K9me3	Monoclonal	CST	13969
H3K9me3	Polyclonal	Abcam	ab8898
H3K27ac	Monoclonal	CST	8173
H3K27ac	Monoclonal	Active Motif	39685
H3K27ac	Polyclonal	Active Motif	39133
H3K27me3	Monoclonal	CST	9733
H3K27me3	Polyclonal	Millipore	07-449

Table 2: Datasets summary.

Antibody	N read pairs (insert size normalized)	Number of Replicates		Region targeted
		Mono	Poly	
H3K27ac	25,808,498	2	2	Transcription start sites, enhancers
H3K27me3	18,616,216	4	3	Repressed regions
H3K4me1	35,524,049	3	2	Enhancers
H3K4me3	9,204,667	4	4	Transcription start sites
H3K9me3	28,456,470	3	2	Repressed regions

Table 3: Comparison of peaks between ChIP-seq datasets derived obtained by monoclonal and polyclonal antibodies.

		Number of Peaks	% Reads In Peaks	% Reads in expected Regions
H3K27ac	MonoRep1	29,320	55.9	88%
	MonoRep2	28,413	51.5	89%
	PolyRep1	33,784	55	80%
	PolyRep2	33,575	54.4	80%
H3K27me3	MonoRep1	10,229	1.1	98%
	MonoRep2	10,148	1.1	98%
	MonoRep3	10,002	1.1	98%
	MonoRep4	10,196	1.1	98%
	PolyRep1	13,984	1.6	98%
	PolyRep2	12,937	1.5	98%
	PolyRep3	18,721	2.3	98%
H3K4me1	MonoRep1	52,118	17.5	30%
	MonoRep2	62,227	25.8	29%
	MonoRep3	54,468	19	34%
	PolyRep1	59,427	25.1	32%
	PolyRep2	58,730	24.7	33%
H3K4me3	MonoRep1	15,002	23.9	93%
	MonoRep2	15,167	26.9	93%
	MonoRep3	15,185	26.7	93%
	MonoRep4	15,053	25.6	93%
	PolyRep1	15,904	33	92%
	PolyRep2	15,982	31.9	91%
	PolyRep3	15,956	31.1	92%
	PolyRep4	16,160	29.9	92%
H3K9me3	MonoRep1	6,083	5.4	74%
	MonoRep2	5,326	5	72%
	MonoRep3	5,533	4.1	63%
	PolyRep1	9,399	5	69%
	PolyRep2	7,411	4.6	68%

Table 4: Overlap of peaks.

	Mono vs Poly	Mono vs Mono	Poly vs Poly
H3K27ac	79%	86%	85%
H3K27me3	11%	11%	13%
H3K4me1	62%	61%	70%
H3K4me3	86%	86%	86%
H3K9me1	21%	22%	27%

The average percentage of peaks that overlap between replicates of the same antibody as compared to monoclonal versus polyclonal antibodies to the same epitope. A peak is considered overlapping if at least half of the peak is covered by a peak in the other dataset.